International Journal of Thermal Sciences 184 (2023) 107998

Contents lists available at ScienceDirect

International Journal of Thermal Sciences

journal homepage: www.elsevier.com/locate/ijts

A discretization method for the characterization of a plate heat exchanger working as evaporator during transient conditions

F. Illán-Gómez *, J.R. García-Cascales, R. Molina-Valverde, F.J.S. Velasco

DITF, ETSI Industrial, Universidad Politécnica de Cartagena, Dr. Fleming s/n, 30202, Cartagena, Murcia, Spain

ARTICLE INFO

Keywords:
Heat exchangers model
Evaporator
Plate heat exchangers

ABSTRACT

In this work, a method for the characterization of a plate heat exchanger working as evaporator is presented. It is based on a one-dimensional discretization of the exchanger, which solves the heat transfer balance equations by means of an iterative methodology based on a heat transfer area converging method. The inputs of the method are the flow rates of the fluids, the inlet enthalpy of the refrigerant, the superheating, and the inlet temperature and pressure of the secondary fluid. Once the inlet pressure of the refrigerant is assumed, pressure drop is calculated in each cell and then enthalpy. The consideration of the proper heat transfer coefficient (HTC) correlations allows the calculation of the heat transfer area, which is after compared to the actual one. The method has been validated by means of a database of 366 experimental data obtained for eight plate heat exchangers working as evaporators by using six different refrigerants, namely R134a, R1234yf, R513A, R744, R290, and R507A. As the method requires suitable correlations for the calculation of the HTC and pressure drop, several correlations for the HTC and Δp found in the literature are studied and the results obtained by using them are presented in terms of the maximum absolute relative deviation (MARD). The results corresponding to the correlation which yields the best results are graphically represented. Finally, the method is used to predict the evaporator performance operating in transient conditions. The results obtained show an excellent agreement with the experimental results collected during the transient operation of a transcritical CO_2 water heater coupled to a storage tank.

1. Introduction

The availability of accurate models for heat exchangers (HEX) is fundamental whenever a thermal system is going to be designed or studied. In this work, the authors are interested in the identification and implementation of an accurate and robust model for the characterization of an evaporator, which in a second stage may be incorporated to the complex model of a water/water heat pump for hot water generation whose dynamical behavior will be analyzed in future works. This analysis will be carried out to evaluate the seasonal performance of different solutions of the system under a certain demand, paying attention to the environmental impact and the primary energy consumption of each solution. This sort of calculation requires a compromise between accuracy and time consumption as these calculations are often carried out yearly with time steps of 1 h or less.

The first step would be to identify the already published models one may find in the existing literature and try to implement any of them. Indeed, there are many models and simulation tools for heat exchangers available. As a first approach, lump parameter models might be used. Usually they are based in LMTD or NTU/ε methods and may result in an iterative procedure if the heat exchanger is divided into several zones. Their description may be found in many heat exchangers books [1,2]. Another approach based on lumped parameter models is bond graphs modeling [3–5]; are recent examples of the application of bond graphs to the simulation of plate heat exchangers (PHE). Other models contemplate the discretization of the heat exchanger into cells/control volumes to which conservation equations are applied. Among them, let us mention for finned-and-tubes heat exchangers the work by Lee and Domanski [6], which introduces a 1D tube-by-tube model which is extended to zeotropic mixtures, Corberán et al. [7] describes SWETLE model which is a finite volume approach that explicitly resolves the 1D momentum and energy equations for each of the cells into which the heat exchanger is divided. Jiang [8], and Jiang et al. [9], similarly to the other references, divides the HEX into segments where the balance conservation equations are applied. These models resulted in the development of codes such as EVAP-COND [10], IMST-ART [11], and CoilDesigner [12] respectively. Recent contributions for microchannel

* Corresponding author.
E-mail address: fernando.illan@upct.es (F. Illán-Gómez).

https://doi.org/10.1016/j.ijthermalsci.2022.107998
Received 21 April 2022; Received in revised form 14 October 2022; Accepted 21 October 2022
Available online 3 November 2022

Nomenclature

A	heat transfer area (m^2)
Bd	Bond number (−)
Bo	boiling number (−)
c_p	specific heat at constant pressure ($J{\cdot}kg^{-1}{\cdot}K^{-1}$)
d_h	hydraulic diameter (m)
f	friction factor (−)
g	gravity constant ($m{\cdot}s^{-2}$)
G	flow velocity ($kg{\cdot}m^{-2}{\cdot}s^{-1}$)
h	enthalpy ($J{\cdot}kg^{-1}$)
h_{fg}	latent heat of vaporization ($J{\cdot}kg^{-1}$)
L	plate length (m)
M	molar mass ($kg{\cdot}kmol^{-1}$)
$\dot{m}$	mass flow rate ($kg{\cdot}s^{-1}$)
$MARD$	mean absolute relative difference (%)
n	number of elements
Nu	Nussel number (−)
p	pressure (Pa)
Pr	Prandtl number (−)
q	heat flux ($W{\cdot}m^{-2}$)
$\dot{Q}$	heat rate (W)
Re	Reynolds number (−)
Ra	average surface roughness (μm)
SH	superheating (°C, K)
t	plate thickness (m)
T	temperature (°C, K)
U	overall heat transfer coefficient ($W{\cdot}m^{-2}{\cdot}K^{-1}$)
$\dot{V}$	volumetric flow ($m^3{\cdot}s^{-1}$)
W	plate width (m)
We	Weber number (−)
x	vapor quality (−)
X	Martinelli parameter (−)

Greeks

α	local heat transfer coefficient ($W{\cdot}m^{-2}{\cdot}K^{-1}$)
β	chevron angle (°)
ε	void fraction (−)
Δ	difference
φ	surface enlargement factor (−)
φ^2	two-phase multiplier (−)
λ	thermal conductivity ($W{\cdot}m^{-1}{\cdot}K^{-1}$)
μ	dynamic viscosity ($N{\cdot}s{\cdot}m^{-2}$)
ρ	density ($kg{\cdot}m^{-3}$)
σ	surface tension (Pa)

Subscripts and superscripts

0	reference state
a	acceleration
cb	convective boiling
cr	critical
eq	equivalent
g	gas, saturated vapor
grav	gravity
i	inlet
l	liquid
lm	log mean
lo	liquid only
m	mean or homogeneous
max	maximum
nb	nucleate boiling
o	outlet
r	refrigerant
red	reduced
sec	secondary fluid
tp	two-phase
v	vapor
w	wall

heat exchangers are the works by Kim and Bullard [13], and Yin et al. [14] which derived a model in which the HEX is divided into cells, which are later analyzed as single heat exchangers. In the first work the authors analyzed an evaporator and in the second a gas cooler. Asinari et al. [15] developed a 3D model which used SEWTLE approach, García-Cascales et al. [16,17] developed a 1D sequential model which is included inside MPower code [18], this model turns into an iterative one when several tube rows are considered, Fronk and Garimella [19] also modeled a new compact HEX design by dividing it into segments and validating the model considering a gas cooler application, Martínez Ballester [20] followed a similar strategy but in addition he included conduction as Asinari et al. did in their work [15]. For their part, Corberán et al. [21] also developed SEWTLE for the analysis of plates heat exchanger with success, Qiao et al. [22] divided the HEX in segments in a generalized way that let them study phase change and maldistribution with high accuracy, this was later improved by Eldeeb et al. [23] by introducing a new algorithm which improves the model speed, Gullapalli [24] used SEWTLE in a generalized rating method which is included in SSP G8 software [25]. This method was later integrated on a steady state Organic Rankine Cycle (ORC) system simulation program capable of simulating a variety of ORC cycles using brazed plate heat exchangers (BPHE) components as heat exchangers [26]. Yoon and Jeong [27] developed a numerical analysis model using a flow network approach to evaluate the thermal-hydraulic performance of a plate heat exchanger. Each channel is modeled as a flow network of unit cells composed by nodes and branches. The node contains the information related to the volume-averaged temperature, pressure and enthalpy of the unit cells, whereas the branches are the flow paths connecting the nodes. The method is able to consider non-uniform flow distribution in both the port-to-channel flow distribution and across-channel flow distribution, and allows determining the local distributions of the temperature, pressure and mass flow rate at a specific location in a channel. Jeong et al. [28] developed a model to investigate the performance of a PHE operating as the evaporator of an ORC system, where the inlet temperature, pressure, and mass flow rate of both fluids were the input parameters.

Some authors have focused their efforts on developing simulation models that can be used for the control of thermal systems. Most of those works are devoted to PHE operating with single-phase fluids (typically water). Among the more recent works, Fratczak et al. [29] suggested a simplified dynamical model which, although according to the authors can be used for design and optimization, is mainly focused on control applications; they validated their model using water on both sides. Similarly, Wang et al. [30] proposed a state space model of a water-to-water PHE and developed a loop-shaping controller based on it which, according to the authors, is superior to a PI controller. He et al. [31] developed a model based on the thermal-electric analogy, which was used in an integrated control method to perform the optimal control of a heat transfer system including both, single-phase heat exchangers and an evaporator. Csurcsia et al. [32] built a polynomial nonlinear space state-based decoupled model to simulate the transient performance of a plate heat exchanger working with water as both cold and hot fluids.

Other recent papers dealing with the simulation of PHE are mainly focused on optimizing the design of these devices. Raja et at [33]. used a multi-objective heat transfer search (MOHTS) algorithm to model and

thermal-hydraulic optimization of water-to-water PHE. Shokouhmand and Hasanpour [34] performed the thermal and hydraulic optimization of a PHE using a multi-objective genetic algorithm known as NSGA-II to obtain the optimal trade-off between effectiveness and pressure drop. They validated their method against a database of 30 experimental tests developed using water both as cold and hot fluids. Dinesh Kumar et al. [35] used the multi objective wale optimization (MOWO) technique to improve the heat transfer and reduce the pressure drop in a water-to-water PHE. Nahes et al. [36] presented a model based on differential balance equations that are discretized using a finite-difference scheme, and used this model for the design optimization of gasketed-plate heat exchangers. Although the authors claim that it can be extended to other alternatives, it has only been proven in applications without phase change. Starace et al. [37,38] and Fiorentino and Starace [39] proposed what they called a "hybrid method", designed to obtain the overall heat exchanger performance starting from micro-scale data obtained from experimental, numerical, or analytical analysis. The method extends those small-scale results to the overall system by dividing the whole heat transfer domain into micro-volumes where regression functions are determined to describe their performance depending on working parameters.

This work is focused on the modeling of plate heat exchanger evaporators in such a way that the method developed can be easily integrated into a dynamic model of a whole refrigeration/heat pump system. Since the evaporation pressure is usually an unknown variable in those systems, contrary to many of the methods previously cited, the method proposed here rather than using the inlet pressure as an input of the method, assumes an initial value for the inlet pressure which is corrected in an iterative process until the method converges. As noted above, they can be analyzed by means of a one or two zone global models but the variability of the HTC in the two-phase zone make them inappropriate if accuracy is being sought. As far as discretization methods are concerned, from the authors' point of view, there are methods in the literature for plate heat exchangers which have been demonstrated to be very accurate (SWETLE, Gullapalli, Yoon and Jeong, and so on) but they also have a high computational cost for their inclusion in a global model for dynamical simulations mostly due to their complexity. Hence, the idea behind this work is to develop a robust and sufficiently simple model, which after including it in a dynamic study does not require a high consumption of computational resources and provides accurate results. Accuracy is searched by discretizing the heat exchanger and fast calculation is fulfilled by reducing the number of variables used, avoiding the use of wall temperatures, accepting as valid a one dimensional study, and using linear interpolation in 2D maps for the evaluation of the thermodynamic properties which are previously calculated following the method presented in Corberán et al. [40].

In this case, the authors have wanted to go further trying to reach higher accuracy by means of discretization methods among which tube-by-tube models for fin-and-tube HEX or cell-by-cell models for plate heat exchanger are good candidates (García-Cascales et al., 2010). Therefore, the model presented in this paper poses a one-dimensional cell-by-cell discretization of the evaporator by applying energy conservation equation to each control volume and solving iteratively until convergence is reached. Although the equations for the heat transfer rate or the pressure drop will be different, the methodology presented is valid for both, condensers and evaporators, as well as for different types of heat exchangers (plate, finned tube, minichannel, etc.) and can be easily integrated into a dynamic model of a whole refrigeration/heat pump system to simulate the performance of the whole system during long-running transient periods with relatively low computational cost. As a previous step to test this capability, the method will be used in the sixth section of this work to analyze the performance of an evaporator operating under long-running transient periods at four different evaporator water inlet temperatures (around 8 h and 1500 different experimental points each test).

This work is structured as follows: firstly, the numerical method proposed to simulate the evaporator is described. The correlations studied for the evaluation of the HTC and the pressure drop are presented. Then, the heat exchangers considered in the experiments, the experimental data and the uncertainty associated with the variables used in the study are shown. Later on, the different tests are evaluated by using the numerical method presented and compared to the experimental data. In the final section, some conclusions are drawn.

2. Evaporator model

The method proposed is a cell-by-cell model, which divides the heat exchanger into a number of cells where the conservation equations of mass, momentum, and energy are posed for each stream and the resulting system of equations is solved by iteration. Like other similar cell-by-cell methods, the method proposed calculates the heat transfer coefficient at each cell to solve the energy equation. Since the method solves the equation system in each cell, unlike LMTD or ε-NTU methods, it not only distinguishes between two-phase and superheated vapor regions but is also capable of distinguishing between different boiling patterns inside the two-phase region. For example, depending on the equations used to model the boiling process, the method distinguishes between nucleate and convective boiling or between microscale and macroscale boiling.

In a refrigeration system typically both evaporation and condensation pressures can not be directly controlled by the user (except in a transcritical refrigeration system, in which the gas cooler pressure is controlled by a back-pressure valve). Instead, evaporation and condensation pressures are indirectly imposed by the operating conditions. For example, if the system is operating at stationary conditions and a sudden increase of the thermal load takes place, the evaporation pressure will normally increase (if the superheating is kept constant) and a new equilibrium state will be reached. Therefore, the objective of any simulation method for an evaporator (or a condenser) should be to obtain, as the first output, the evaporation (or condensation) pressure.

Apart from the geometrical characteristics of the heat exchanger, that is, the number of plates, plate width W, plate length L, and, depending on the correlation used, chevron angle β, in the case of an evaporator, the variables more usually considered as inputs of any model are the mass flow rate of refrigerant $\dot{m}_r$ (which is imposed by the compressor and depends, besides the characteristics compressor, on the evaporation and condensation pressure), the inlet enthalpy of refrigerant h_{ri} (which depends on the refrigerant thermodynamic state at the condenser outlet), the superheating SH, (which is imposed by the expansion device, typically a thermostatic expansion valve or an electronic expansion valve), as well as the inlet volume flow rate of secondary fluid $\dot{V}_{seci}$ and the inlet temperature of secondary fluid T_{sec}., which usually depend on the application.

The method presented here will determine the evaporation pressure from all those inputs and, once the evaporation pressure is known, other interest variables will be obtained (heat rate, secondary fluid output temperature, etc.). In the model presented, the evaporator is considered vertical, and the fluids are considered to flow counter-currently as in Fig. 1. First of all, let us divide the heat exchanger vertically into 2n+1 nodes and 2n elements as in Fig. 2. These elements have a constant width, which coincides with the plates width and a length (height) that is denoted as L_j. The thermophysical properties will be defined in each node, p_j, T_j, h_j, and so on. All thermodynamic properties are evaluated by using Refprop [41]. Furthermore, in each element, a pressure difference Δp_j, a quality difference Δx_j, a heat transfer area A_j, and the heat exchanged $\dot{Q}_j$ are defined.

In a real system, evaporation pressure is imposed by the secondary fluid conditions so "a priori" it is unknown and as a first step it is to be assumed. Considering the input variables of the problem, let us assume inlet refrigerant pressure, p_{ri}

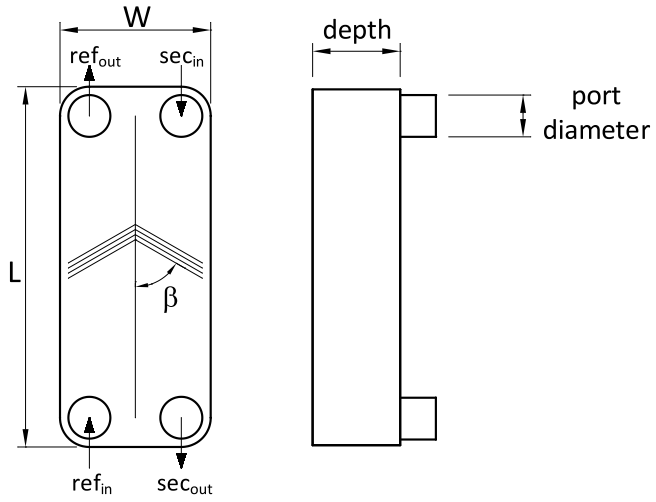

Fig. 1. Schematic diagram of the plate heat exchanger considered.

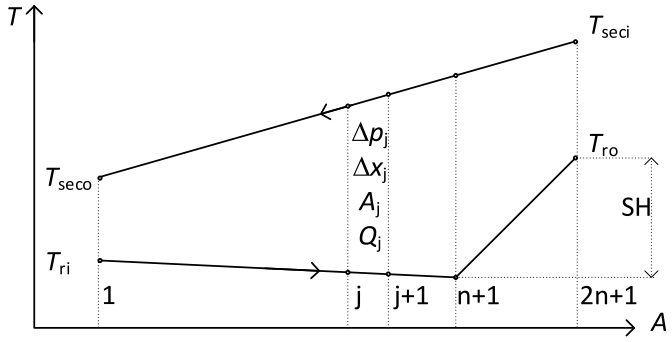

Fig. 2. Description of the divisions considered on the temperature profile in the evaporator.

$$p_{ri} = \frac{p_{low} + p_{high}}{2} \tag{1}$$

where $p_{high} = p_{sat}(T_{seci})$ and $p_{low} = p_{sat}$ (at an arbitrary low T, i.e. $-40\ ^{\circ}C$), now with this pressure and the inlet enthalpy h_{ri} let us evaluate the values of quality x_i and temperature T_{ri} at the inlet. On doing so, let us define an average quality difference

$$\Delta x_r = \frac{1 - x_{r1}}{n} \tag{2}$$

and an average length difference

$$\Delta L = \frac{plate\ height}{2n} \tag{3}$$

The idea of the method resides in imposing an equal quality difference in each of the n two-phase elements $\Delta x_j = \Delta x_r$ and a variable length which initially will be assumed to be $L_j = \Delta L$. Then, the heat exchanger is analyzed sequentially by starting from the inlet (two-phase flow) so pressure drop of element j, Δp_j is firstly evaluated considering the value of the thermodynamic variables in node j and the length of element j, L_j after that pressure of node j+1 is calculated and thus enthalpy $h_{j+1} = h(p_{j+1}, x_{j+1})$ and the heat exchanged in the jth element

$$p_{j+1} = p_j - \Delta p_j \tag{4}$$

$$\dot{Q}_{rj} = \dot{m}_r \left(h_{rj+1} - h_{rj}\right) \tag{5}$$

Once the saturation line is reached, the superheating zone is divided into n elements with the same temperature difference ΔT_j so:

$$\Delta T = \frac{SH}{n} \tag{6}$$

and an initial length $L_j = \Delta L$. Again, in this zone, the pressure drop is evaluated for each element, which let us calculate pressure, enthalpy of the nodes and heat exchanged in the different elements.

As the heat exchanged in all the elements is known, the temperature at all nodes in the secondary fluid side may be calculated,

$$T_{secj} = T_{secj+1} - \frac{\dot{Q}_{rj}}{c_{psec}\dot{m}_{sec}} \tag{7}$$

At this point, the thermodynamic state of all nodes is known on both sides (refrigerant and secondary fluid side). Considering average values for each element, the overall HTC U_j is evaluated as:

$$U_j = \left(\frac{1}{\alpha_{rj}} + \frac{t}{\lambda_w} + \frac{1}{\alpha_{secj}}\right)^{-1} \tag{8}$$

then the area corresponding to element j is recalculated

$$A_j = \frac{\dot{Q}_{rj}}{U_j \Delta T_{lmj}} \tag{9}$$

and so its corresponding length

$$L_j = plate\ height \frac{A_j}{A_{total}}. \tag{10}$$

Now the calculated height (or calculated area) of the heat exchanger, $\sum_{j=1}^{2n} L_j$ is compared with the actual plate height (total area) and if they are different in more than an arbitrarily small value (E) the process is repeated with these new element lengths until the process converges, then a new refrigerant inlet pressure is assumed considering expression (2) but redefining

$$p_{high} = p_{ri}\ if\ A_{total} > A_{calculated}$$

$$p_{low} = p_{ri}\ if\ A_{total} < A_{calculated} \tag{11}$$

As is noticed in Fig. 3, the methodology relies on the proper evaluation of the heat transfer coefficients and pressure drop in each cell at both sides, the refrigerant and the secondary fluid.

The method presented has certain similarities with the one proposed by Simon and Bandhauer [42]. They used a heat exchanger discretization in which the control volumes are defined by fixing the heat duty of the control volume and calculating the required heat transfer area. The heat duty in each region (subcooled, two-phase, and superheated regions) is defined by the refrigerant enthalpy difference between the inlet and outlet of each phase region, multiplied by the refrigerant mass flow rate through a single channel set and divided by the number of control volumes in the phase region. In their model, the sum of the lengths of all control volumes, calculated based on the heat duty, is compared to the actual experimental length in order to determine the accuracy of the model. However, unlike the model presented here, instead of seeking the evaporation pressure, they use the refrigerant inlet pressure as an input, and their method is not iterative. Their approach is based on the search for the combination of heat transfer correlations (for the water side and each refrigerant region) that provides the value of the total length closest to the actual one.

In the following sections, some correlations are considered, the method presented is tested, and the results obtained are compared to some experimental data.

3. Heat transfer

The heat transferred in the heat exchanger is characterized by means of suitable HTC correlations in the evaporation (two-phase flow) and superheating zones (single-phase flow) in the refrigerant side and in the

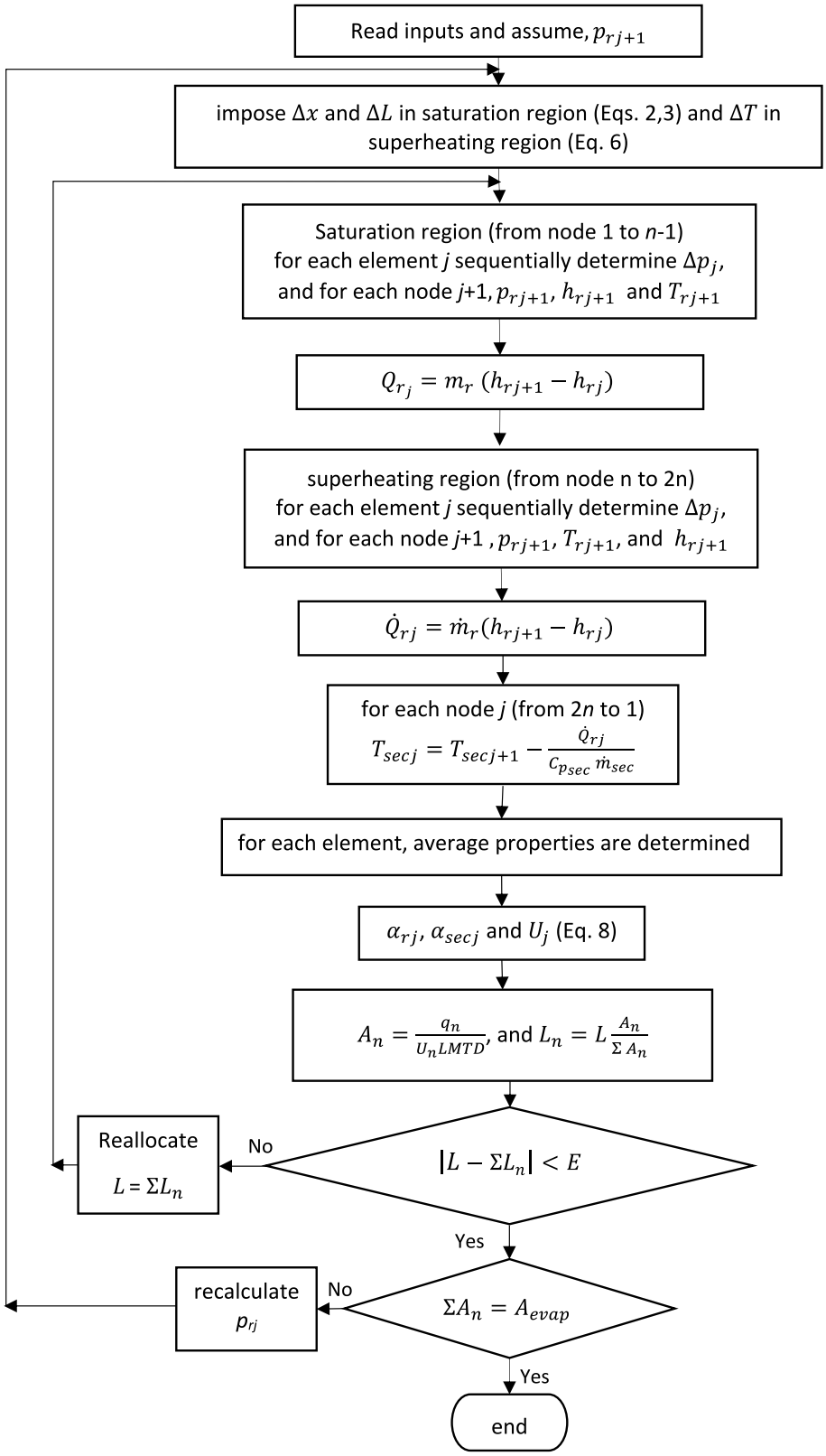

Fig. 3. Flow chart of the methodology presented.

secondary fluid side (single-phase flow).

In both cases, the amount of correlations derived by authors is constantly increasing. Regarding single-phase, over the years, several authors have made an extensive study of the correlations available in the literature for the analysis of single-phase heat transfer in heat exchanger comparing some of them (i.e. Claesson [43], García-Cascales et al. [44]). As was pointed out there, force convection heat transfer coefficient is frequently correlated as a Dittus-Boelter type correlation where the different coefficients usually depend on the plate pattern and geometrical parameters.

As far as boiling is concerned, it is well known that this is dominated by two phenomena: convective and nucleate boiling. It is accepted that at high heat fluxes and low qualities, nucleate boiling is more influential than convective boiling. For small heat exchangers, nucleate boiling dominates and the effect of gravity is almost negligible. Bearing this in mind, the two-phase HTC usually considers both phenomena and is frequently formulated by using superposition, asymptotic or enhancement models. In order to include both effects, convective boiling and nucleate boiling, the first two types of models calculate the HTC as:

$$\alpha_r = \left\{\alpha_{nb}^n + \alpha_{cb}^n\right\}^{1/n} \tag{12}$$

where n is the order of the asymptotic model. When $n = 1$, the model is in fact a superposition model, when n takes large values ($n \approx \infty$) the HTC tends to take the higher value between the convective boiling and the nucleate boiling, whereas other values for n give an asymptotic power law model that assures a smooth transition between the nucleate dominated boiling and the convective dominate boiling.

On the other hand, the enhancement models, instead correct a single-phase correlation with an enhancement factor that accounts the effect of other variables, heat transfer, heat flux, vapor quality, saturation pressure, and so on. Unlikely tubes, in a plate heat exchanger is not usual to consider the flow pattern.

Amalfi et al. [45] made an extensive review of HTC and frictional pressure drop models in plate heat exchangers. According to the authors, most HTC models are based only on their own specific experimental data and one or two working fluids, without inclusion of independent data. No clear criteria is available to determine the transition between nucleate boiling and convective boiling and, as a result, there is no widely validated correlation available in the literature to predict the flow boiling heat transfer coefficient in PHEs. In the second part of their work, Amalfi et al. [46], the authors performed a dimension analysis coupled with a multiple regression analysis, in order to correlate the two-phase Nusselt number (Nu_{tp}) to other non-dimensional groups. They adopted the Kew and Cornwell [47] transition criteria from macro to microscale, that, according to Kew and Cornwell, occurs for tubular geometries at a Bond number Bd = 4, being the Bond number calculated as:

$$\mathrm{Bd} = \frac{(\rho_l - \rho_v)\cdot g \cdot d_h^2}{\sigma} \tag{13}$$

Where σ is the fluid surface tension.

Consequently, Amalfi proposed two different correlations to predict the two-phase Nusselt number depending on the experimental Bond number value. When the experimental Bond number is lower than 4 (microscale), the two-phase Nusselt number is associated to the homogeneous Weber number (We_m), Boiling number (Bo), liquid/vapor density ratio ($\rho^* = \rho_l/\rho_v$), and the reduced chevron angle ($\beta^* = \beta/\beta_{max}$) according to the expression:

$$\mathrm{Nu}_{tp} = 982\cdot\beta^{*1.011}\cdot\mathrm{We}_m^{0.315}\cdot\mathrm{Bo}^{0.320}\cdot\rho^{*-0.224} \tag{14}$$

where the homogeneous Weber number is:

$$\mathrm{We}_m = \frac{G^2\cdot d_h}{\rho_m\cdot\sigma} \tag{15}$$

And the Boiling number is:

$$\mathrm{Bo} = \frac{q}{G\cdot h_{lv}} \tag{16}$$

where q is the heat flux, h_{lv} is the latent heat of vaporization, and G is the mass flux.

When the Bond number is higher than or equal to 4 (macroscale), the homogeneous Weber number is replaced by the vapor Reynolds (Re_v) and the liquid only Reynolds (Re_{lo}) numbers, and the Bond number also enters in the correlation:

$$\mathrm{Nu}_{tp} = 18.495\cdot\beta^{*0.248}\cdot\mathrm{Re}_v^{0.135}\cdot\mathrm{Re}_{lo}^{0.351}\cdot\mathrm{Bd}^{0.235}\cdot\mathrm{Bo}^{0.198}\cdot\rho^{*-0.223} \tag{17}$$

where the vapor Reynolds is:

$$Re_v = \frac{G\cdot x\cdot d_h}{\mu_v} \tag{18}$$

And the liquid only Reynolds is:

$$Re_{lo} = \frac{G\cdot d_h}{\mu_l} \tag{19}$$

According to the authors, the model proposed was validated against 1903 experimental data points obtained from literature, including a wide range of operating conditions, plate designs, and fluids, providing a mean absolute error of 22.1% that improved all existing models tested by the authors.

Almost simultaneously with Amalfi's paper, Longo et al. [48] presented a new HTC model for saturated refrigerant boiling inside BPHEs based on a large experimental data-base with results for different refrigerants, including pure and blended high, medium, and low pressure HFCs, hydrocarbons and HFOs, which afterwards they compared with other lab data to assess its generality. Thus, their proposal is to evaluate the two-phase HTC as the maximum of the convective and the nucleate boiling contributions

$$\alpha = \max(\alpha_{nb}, \alpha_{cb}) \tag{20}$$

Being the convective boiling calculated by means of

$$\alpha_{cb} = 0.112\varphi\frac{\lambda_l}{d_h}\mathrm{Re}_{eq}^{0.8}\mathrm{Pr}_l^{1/3} \tag{21}$$

where φ is the enlargement factor given by the quotient of the actual area and the projected area, Re_{eq} is the equivalent Reynolds number and Pr_l is the liquid Prandtl number.

The equivalent Reynolds number is defined as:

$$\mathrm{Re}_{eq} = \frac{G_{eq}d_h}{\mu_l} \tag{22}$$

where:

$$G_{eq} = G\left[(1-x) + x\left(\frac{\rho_l}{\rho_v}\right)^{0.5}\right] \tag{23}$$

The nucleate boiling is calculated by means of:

$$\alpha_{nb} = C_{nb}\varphi C_{Ra}\alpha_0 F(p_{red})\left(\frac{q}{q_0}\right)^n \tag{24}$$

where $C_{nb} = 0.58$, $n = 0.467$, α_0 is the reference value for $p_{r0} = 0.1$, $q_0 = 20$ kW m^{-2}, $Ra_o = 0.4$ μm, the function accounting for the effect of reduced pressure $F(p_{red})$ is given by:

$$F(p_{red}) = 1.2p_{red}^{0.27} + \left(2.5 + \frac{1}{1-p_{red}}\right)p_{red} \tag{25}$$

and:

$$C_{Ra} = \left(\frac{Ra}{0.4\mu\mathrm{m}}\right)^{0.1333} \tag{26}$$

Finally, despite being originally developed for nucleate pool boiling, several authors have reported that the use of Cooper's correlation provides good agreement with experimental data in plate heat exchangers. According to Copper [49], the HTC for nucleating boiling can be obtained as:

$$\alpha_r = 55p_{red}^{0.12-0.2\ log_{10}\ Ra}\left(-log_{10}p_{red}\right)^{-0.55}M^{-0.5}q^{0.67} \tag{27}$$

where M is the fluid molar mass, q the heat flux, Ra the surface

roughness, and p_{red} the reduced pressure, calculated as the ratio between the actual fluid pressure and its critical pressure (p_{cr}):

$$p_{red} = p/p_{cr} \tag{28}$$

According to Claesson [50], his experimental data showed good agreement with a modified Cooper's correlation obtained by simply multiplying Cooper's expression by a factor of 1.5. García-Cascales et al. [44], Longo and Gasparella [51], and Longo [52] also reported good agreement with the original Cooper correlation, without the need to correct it.

4. Pressure drop

Two-phase pressure drop is the evaluated as the sum of the components corresponding to acceleration, gravity (static head), friction in the heat exchanger, and in the inlet, and outlet manifolds.

Pressure losses due to acceleration are evaluated with:

$$\Delta p_a = G^2 \cdot \Delta x \cdot \left(1/\rho_{out} - 1/\rho_{in} \right) \tag{29}$$

where Δx is the quality difference between the input and the output and $\rho_{in/out} = \varepsilon_{in/out}\rho_g + (1 - \varepsilon_{in/out})\rho_l$

The static head is determined with the following expression $\Delta p_{grav} = \rho \cdot g \cdot L$, where density is the average two-phase density in the case of two-phase flow:

$$\Delta p_{grav} = \left(\frac{x}{\rho_v} + \frac{(1-x)}{\rho_l} \right)^{-1} \cdot g \cdot L \tag{30}$$

Pressure drop in the manifolds is calculated by means of:

$$\Delta p_{man} = 1.5 \cdot \frac{G^2}{2 \cdot \rho_m} \tag{31}$$

Where ρ_m is the mean density, obtained as $\rho_m = \left(\frac{x}{\rho_v} + \frac{1-x}{\rho_l} \right)^{-1}$.

The friction component is often calculated by considering a separated model in such a way that this is predicted applying a multiplier to the single-phase pressure drop (gas o liquid) in the tube:

$$\Delta p_{tp} = \Delta p_l \cdot \varphi_l^2 \tag{32}$$

The more common approach correlates the two-phase multiplier with the Martinelli parameter using the Chisholm expression (Chisholm, 1967):

$$\varphi_l^2 = 1 + \frac{C}{X} + \frac{1}{X^2} \tag{33}$$

where the Martinelli parameter is given by $X^2 = (dp/dz)_l / (dp/dz)_v$. In the existing literature, there are different proposals for the Chisholm parameter C, which range from single values [53] to different expressions that correlate this with Reynolds number and/or the Martinelli parameter [50], and Froude number [24].

In addition to previous models, other authors such as Jokar et al. [54] have proposed expressions for the two-phase friction factor when studying the boiling of R134a, so the two-phase frictional pressure drop is calculated by means of the two-phase Fanning expression:

$$\Delta p_{tp} = f_{tp} \cdot \frac{2 \cdot L \cdot G^2}{d_h \cdot \rho_m} \tag{34}$$

being the friction factor based on liquid Reynolds number:

$$f_{tp} = 3.521 \cdot 10^4 \cdot \mathrm{Re}_l^{-1.35} \cdot C_x^{-1} \tag{35}$$

and vapor quality through the factor:

$$C_x = (1-x) + x \cdot \left(\frac{\rho_l}{\rho_v} \right)^{0.5} \tag{36}$$

The authors reported an average standard deviation of about 46%.

More recently, Huang et al. [55] derived a correlation with a mean absolute error of 6.7% considering data of R134a and R507A, thus, the two-phase friction factor is given by:

$$f_{tp} = \frac{3.81 \cdot 10^4 \cdot F_{R,f}}{\mathrm{Re}_{tp}^{0.9} \cdot (\rho_l/\rho_v)^{0.16}} \tag{37}$$

where $Re_{tp} = G \cdot d_h / \mu_{tp}$, the two-phase viscosity is given by $\mu_{tp} = \rho_m \cdot [x \cdot \mu_v / \rho_v + (1-x) \cdot \mu_l / \rho_l]$, and $\rho_m = [x/\rho_v + (1-x)/\rho_l]^{-1}$.

$F_{R,f}$ is a geometrical parameter $F_{R,f} = 0.183 \cdot R^2 - 0.275 \cdot R + 1.1$, being $R = \beta/30$, and β is the corrugation angle.

Longo et al. [52] correlated the frictional pressure drop with the kinetic energy per unit volume deriving the following expression:

$$\Delta p_{tp} = L \cdot 5.25 \cdot \frac{G^2}{2\rho_m} \tag{38}$$

Similarly to what they did for the HTC, Amalfi et al. [46] performed a dimension analysis coupled with a multiple regression analysis, in order to correlate the two-phase friction factor (f_{tp}) to other non-dimensional groups. They proposed the following correlation:

$$f_{tp} = C \cdot 15.698 \cdot \mathrm{We}_m^{-0.475} \cdot \mathrm{Bd}^{0.255} \cdot \rho^{*-0.571} \tag{39}$$

where the parameter C depends on the reduced chevron angle according to the expression:

$$C = 2.125 \cdot \beta^{*9.993} + 0.955 \tag{40}$$

Single-phase pressure drop may be calculated by means of Fanning equation as:

$$\Delta p_l = f \cdot \frac{2 \cdot L \cdot G^2}{d_h \cdot \rho_m} \tag{41}$$

An expression for the single-phase friction factor in plate heat exchangers was proposed by Jokar et al. [54]. The Fanning friction factor is given by:

$$f = 6.431 \cdot \mathrm{Re}^{-0.25} \tag{42}$$

Gullapalli [24] derived an equation for the Darcy friction factor ($f_{\mathrm{Darcy}} = 4 \cdot f_{\mathrm{Fanning}}$) of the form:

$$f = \sum_{i=0}^{3} \sum_{j=0}^{3} C_{ij} \cdot \mathrm{Re}^{-i} \cdot \beta^j \tag{43}$$

the value of the different parameters may be found in Gullapalli reference. Some adjustment parameters are not given which makes the correlation impossible to be used.

5. Validation

A set of 366 experimental data, collected in our own experimental facilities as well as from the open literature, has been used for the validation of the numerical method. Test conditions include six different refrigerants (R134a, R1234yf, R513A, R507A, R290, and R744), eight different plate heat exchangers, and variable operating conditions (different superheating degree, secondary fluid flow rate, or inlet quality). All tests were collected under stationary operating conditions.

In order to validate the method, the results of those tests have been compared to those obtained with the method, which takes as inputs the geometrical information of the heat exchangers and some of the operating conditions of the tests. The geometrical information provided by the heat exchangers' manufacturers, summarized in Table 1, is in

Table 1
Geometrical data of the heat exchangers according to the manufacturers.

Data set	Author	Plate heat exchanger main characteristics						
		Model	Number of plates	Height (m)	Width (m)	Heat transfer area (m^2)	Channels according to the fluid	Chevron angle (°)
1	Illán-Gómez et al. [56]	Swep B8TH	20	0.317	0.076	0.414	9/refrigerant	60/60[a]
2							10/water	
3	Velasco et al. [57]							
4	Illán-Gómez et al. [58,59]	Swep BX8T	26	0.315	0.073	0.552	12/refrigerant	60/60[a]
							13/water	
5	Martínez [60]	Swep V80	26	0.526	0.119	1.44	12/refrigerant	60/60[a]
							13/water	
6		Swep B80	26	0.526	0.119	1.44	12/refrigerant	60/60[a]
							13/water	
7		Swep B27	28	0.524	0.117	1.59	13/refrigerant	60/60[a]
							14/water	
8 & 11	Huang [61]	Danfoss B3-95-24-H	24	0.607	0.18	2.09	11/refrigerant	60/60
							12/water	
9 & 12		Danfoss B3-95-24-L						28/60
10 & 13		Danfoss B3-95-24-M						28/28

[a] Data unknown, value assumed.

general limited. For example, chevron angle is in most cases unknown and, when needed, it has been assumed 60°. Similarly, absolute roughness is also unknown and has been assumed 0.4 μm. The operating conditions of the experimental tests used as inputs of the numerical method are the inlet enthalpy of the refrigerant, the superheating, the inlet temperature of the secondary fluid, and the mass flow rate of the refrigerant and the secondary fluid. This information, summarized in Table 2, has been obtained from our own experimental tests as well as from the open literature. In all cases the secondary fluid is water, whose inlet pressure has been assumed 1.1 bar.

In the calculations performed in this paper, heat transfer and pressure drop for single-phase flow, both in the secondary fluid side, and in the superheated refrigerant side, have been characterized by Qiao et al. [22], and Churchill [62] correlations respectively.

For all cases, two-phase flow frictional pressure drop has been evaluated using equation (37) proposed by Longo et al. [52]. Limited information about the experimental pressure drop is accessible; in fact, this value is not available for the experimental tests performed using R290. In general, the total pressure drop is very low, always in the range of 3–5 kPa for the tests performed in our own facilities (data sets 1–4), and in the range −0.4-7 KPa for the tests performed in Huang's facility (data sets 8–13). Therefore, the saturation temperature drop is very small and has very little impact on the heat exchanger heat transfer process. Due to the limited availability of experimental pressure drop information, and the very small pressure drop reported when accessible, the set of experimental data is not appropriate for the validation of the method and therefore has not been presented here.

Although there are many different two-phase flow HTC correlations available in the literature, most of them were developed using a limited amount of experimental data. Since they were developed and validated by the authors using the widest ranges of different fluids, heat exchanger's geometries, and operating conditions, the correlations developed by Amalfi and by Longo were initially chosen as the two best options to characterize the heat transfer process in the numerical method presented in this work. Due to the good agreement to experimental data reported in previous works, it was found interesting to compare those correlations to Cooper's correlation.

Fig. 4 shows the comparison between the numerical method, using these three correlations, and the experimental results, for the 366 experimental data analyzed. Fig. 4a plots the inlet pressure and Fig. 4b plots the heat transfer rate. Due to the much higher saturation pressure of R744 compared to all the other refrigerants, pressure comparison has been made in a logarithmic basis. As Fig. 4 shows, all three correlations perform similarly, and the numerical method proposed is able to provide a very accurate prediction of the performance of all heat exchangers modeled using any of those three correlations.

In order to establish a clearer comparison among the performance of the three correlations, Table 3 summarizes the Mean Absolute Relative

Table 2
Experimental test conditions according to the authors.

Data set	Author	Operating conditions						
		Fluid	x_i (−)	SH (K)	T_{seci} (°C)	p_{evap} (bar)	$\dot{m}_{sec}$ (kg·s^{-1})	$\dot{m}_r$ (kg·s^{-1})
1	Illán-Gómez et al. [56]	R134a	0.2–0.32	7.4–9.3	12	3–3.2	0.08–0.11	0.012–0.015
2		R1234yf	0.22–0.38	6.3–12	12	3.1–3.4	0.08–0.11	0.015–0.018
3	Velasco et al. [57]	R513A	0.23–0.37	10.4–12.6	12	3.2–3.4	0.086–0.11	0.014–0.016
4	Illán-Gómez et al. [58,59]	R744	0[a]-0.82	0.1–10.9	10–30	34.3–56.6	0.22–0.42	0.02–0.049
5	Martínez [60]	R290	0.24–0.29	1.6–8.2	12	4.9–5.1	0.64–0.7	0.048–0.051
6			0.29–0.32	0.3–1.4	15	5.3–5.4	0.6–0.65	0.05–0.052
7			0.27–0.28	0.5–1.9	10	4.6–4.8	0.55–0.57	0.042–0.044
8	Huang [61]	R134a	0[a]	0.21–0.92[b]	13.7–16	3.6–4.5	0.5–0.8	0.024–0.13
9				0.2–0.95[b]	13.8–15.9	3.6–4.5	0.5–0.8	0.025–0.12
10				0.2–0.9[b]	13.8–15.9	3.8–4.6	0.5–0.8	0.025–0.12
11		R507A		0.2–0.62[b]	16.3–16.6	8–8.7	0.8	0.07–0.13
12				0.17–0.64[b]	16.2–16.3	8.2–8.8	0.8	0.07–0.13
13				0.16–0.66[b]	16.2–16.3	8.4–9.2	0.8	0.076–0.135

[a] Saturated liquid.
[b] Outlet quality.

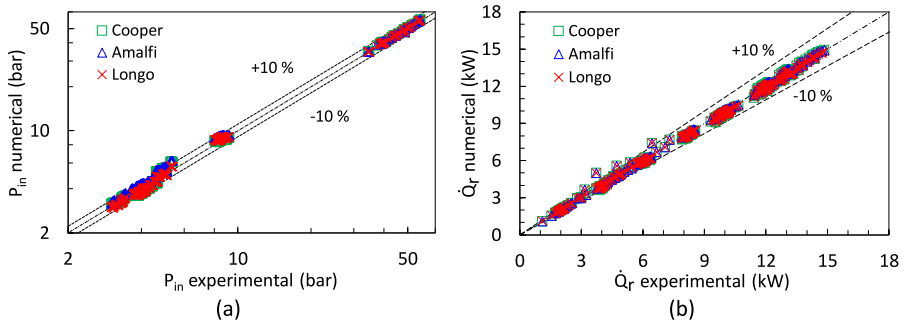

Fig. 4. Two-phase heat transfer models comparison.

Table 3
MARD (%) obtained by using Amalfi (A), Cooper (C), and Longo (L) correlations.

Data set	Fluid	p_{ri} (bar)			$\dot{Q}_r$ (kW)			T_{seco} (K)		
		A	C	L	A	C	L	A	C	L
1	R134a	6.06	3.32	2.31	0.83	0.52	0.16	0.07	0.06	0.05
2	R1234yf	5.60	3.44	0.64	1.46	1.08	0.50	0.02	0.01	0.01
3	R513A	0.95	1.20	3.42	0.19	0.13	0.24	0.08	0.08	0.08
4	R744	1.60	1.14	0.85	2.49	2.35	2.29	0.07	0.07	0.07
5	R290	9.97	8.49	1.74	1.28	1.08	0.24	0.02	0.02	0.00
6	R290	16.53	14.32	6.80	2.29	1.97	1.00	0.04	0.03	0.02
7	R290	13.77	11.37	2.83	1.76	1.45	0.40	0.03	0.03	0.01
8	R134a	7.34	3.37	2.15	0.10	1.96	1.59	0.01	0.03	0.02
9	R134a	4.93	5.49	4.33	0.11	2.56	2.21	0.01	0.03	0.03
10	R134a	3.24	7.05	5.93	0.11	2.56	2.21	0.01	0.03	0.03
11	R507A	8.98	4.20	5.79	1.00	2.04	1.68	0.01	0.03	0.02
12	R507A	6.82	2.11	3.66	9.43	10.03	0.68	0.05	0.06	0.01
13	R507A	6.04	3.36	1.84	0.52	2.38	1.78	0.01	0.03	0.02
1–13	All	5.79	4.76	3.33	1.24	2.48	1.65	0.03	0.04	0.03

Deviation (MARD) values obtained for the evaporator inlet pressure (p_{ri}), the heat transfer rate ($\dot{Q}_r$), and the secondary fluid outlet temperature (T_{seco}), after simulating each set of experimental data. For each X parameter evaluated, MARD is calculated as:

$$MARD\ (\%) = \frac{100}{N}\sum_{i=1}^{N}\left|\frac{X_{model}(i) - X_{experimental}(i)}{X_{experimental}(i)}\right| \tag{44}$$

According to the results presented in Table 3, the Amalfi correlation provides the best prediction of the evaporator heat transfer rate, the Longo correlation provides the best prediction for the evaporator inlet pressure, whereas the Cooper correlation remains in an intermediate position in both cases. There are no important differences among the different fluids or heat exchanger geometries analyzed.

Since the Longo correlation performs clearly better for predicting the evaporation pressure and is only slightly worse than the Amalfi correlation for predicting the heat transfer rate, it has been finally chosen as the correlation used in the numerical method to obtain all the results presented below.

Figs. 5 and 6 show the main results obtained using the numerical method, compared to those experimentally measured, desegregated according to the data set. According to Fig. 5a, all inlet pressure values calculated by the method fall into a ±10% deviation range, although, as can be appreciated in Fig. 5b, for data sets 6, 9, 10, 11, and 12, where the MARD is higher, a deviation around ±5% in the evaporation pressure can lead to deviations around ±2 °C in the saturation temperature.

As Fig. 6a shows, the deviation in the heat transfer rate is lower than 10% in almost all cases. In fact, in 357 out of 366 point, the deviation is lower than 5% and there are only 4 point, all corresponding to data set 4, in which the deviation is higher than 10%. According to Fig. 6b, despite this deviation on the heat transfer rate, there is only 1 point in which the deviation in the secondary fluid outlet temperature is higher than 1 °C.

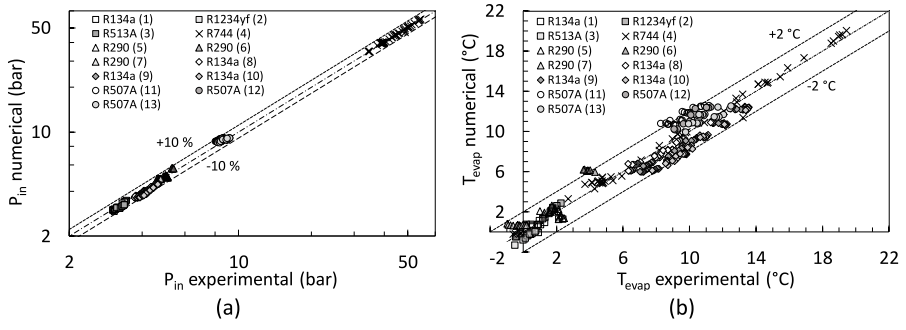

Fig. 5. Refrigerant inlet pressure (a) and temperature (b).

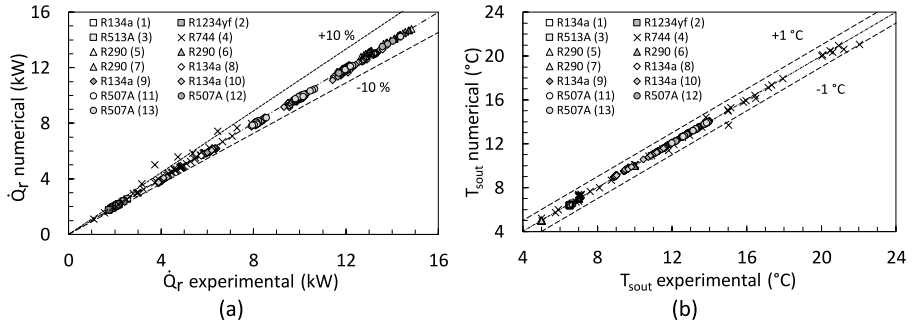

Fig. 6. Refrigerant evaporation temperature.

6. Transient simulation

Once it has been validated against stationary data, this section presents the results obtained using the numerical method to predict the evaporator performance operating in transient conditions. Experimental data obtained during the transient operation of a transcritical CO_2 water heater coupled to a storage tank [63] have been used for this purpose. Four different tests were performed at four different evaporator water inlet temperatures, namely 5 °C, 10 °C, 15 °C, and 20 °C, and constant water mass flow rate (0.54 kg s^{-1}). During all those tests, the system heats up the water contained in a storage tank, from an initial temperature of 10 °C up to a final temperature of 60 °C. The duration of each test is different, ranging from 7.2 h (test at 20 °C) to 11.9 h (test at 5 °C), but the sampling period is the same in all cases (20 s).

Fig. 7a shows the time evolution of the variables taken as input for the numerical method for the test performed with an evaporator water inlet temperature of 10 °C. As the test evolves, the water contained in the tank heats up, enters the gas cooler warmer and the refrigerant leaves the gas cooler (and enters the evaporator) with higher enthalpy, as shown in Fig. 7a. Since the system operated at variable (optimal) gas cooler pressure, as the temperature of the domestic hot water (DHW) contained in the tank increases, the gas cooler pressure changes as can be seen in Fig. 7b. Initially, that pressure increases gradually until it reaches its maximum value and then, it decreases in order to keep the compressor discharge temperature below 150 °C. Since, as Fig. 8a shows, the evaporation pressure is almost constant, the compression ratio initially increases up to a maximum value and then decreases. Consequently, as shown in Fig. 7a, the refrigerant mass flow rate displaced by the compressor decreases gradually until it stays relatively stable towards the final part of the test. The superheating degree stays relatively stable during the entire test at around 7 °C.

Fig. 8a shows the comparison between the time evolution of the evaporation temperature calculated by the numerical method and that experimentally measured, for two different tests. As it can be seen, in the case of the test performed with the higher water inlet temperature (20 °C) the numerical method provides an almost perfect prediction of the evaporation temperature for the whole duration of the test (7.2 h, almost 1300 different experimental points). In the case of the test at 10 °C (8.7 h, more than 1550 experimental points), there is a higher difference between the predicted and measured evaporation temperature, although only during the first 5 min of the test, that difference is slightly higher than 1 °C. From minute five, that difference decreases gradually until it reaches values lower than 0.2 °C around the middle of the test. As Fig. 8b shows, the prediction of the evaporator heat transfer rate is almost perfect during the whole duration of both tests.

Finally, Figs. 9–11 shown the comparison between experimental data and numerical method results for the evaporator inlet pressure (Fig. 9), evaporator heat transfer rate (Fig. 10), and secondary fluid outlet temperature (Fig. 11), for all the four transient tests analyzed.

The maximum deviation for the evaporator inlet pressure is 3.7% (more than 6300 points simulated), with a MARD of 0.52%. In the case of the heat transfer rate, the results are even better, with a maximum deviation lower than 0.4% and a MARD of only 0.08%. The maximum deviation for the secondary fluid outlet temperature is 1.24 °C, and the mean deviation is 0.24 °C. Since this outlet temperature is relatively low and, in many cases near 0 °C, the MARD is high when evaluated in degrees Celsius (3.97%), but is very low if it is evaluated in kelvin (0.08%).

7. Conclusions

In this work, a method for the characterization of a plate heat exchanger working as evaporator has been presented. It is based on a one-dimensional discretization of the exchanger, which permits solving the heat transfer balance equations by means of an iterative methodology based on a heat transfer area converging method. The method takes as input parameters the mass flow rate of refrigerant, its inlet enthalpy, the superheating degree, the mass flow rate of the secondary fluid, and its inlet temperature. The solving procedure consists of assuming an inlet pressure for the refrigerant, which permits evaluating the pressure drop in each cell and then, the enthalpies at each node, which finally allows calculating the heat exchanged in each element. The evaluation of the HTC in the elements permits determining the heat transfer area,

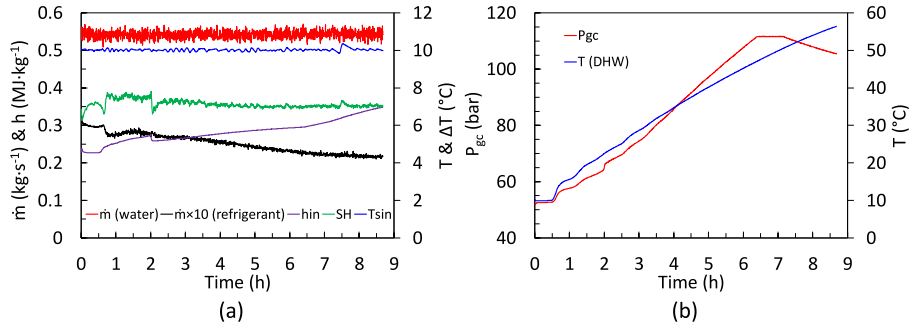

Fig. 7. Input variables time evolution for transient test with evaporator water inlet temperature of 10 °C (a) and gas cooler operating conditions time evolution (b).

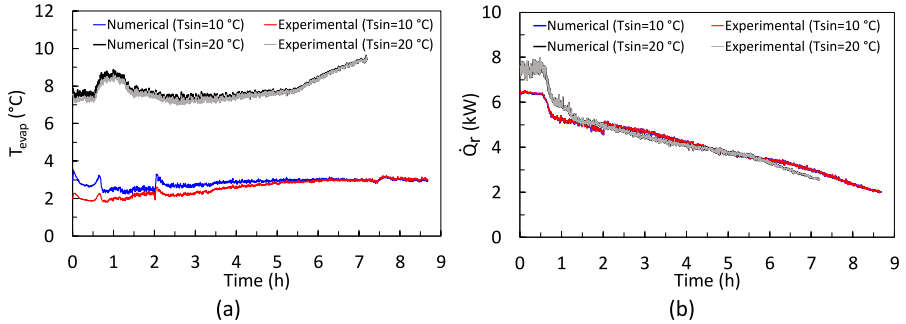

Fig. 8. Simulated evaporation temperature (a) and heat transfer rate (b) time evolution compared to experimental data for two different transient tests.

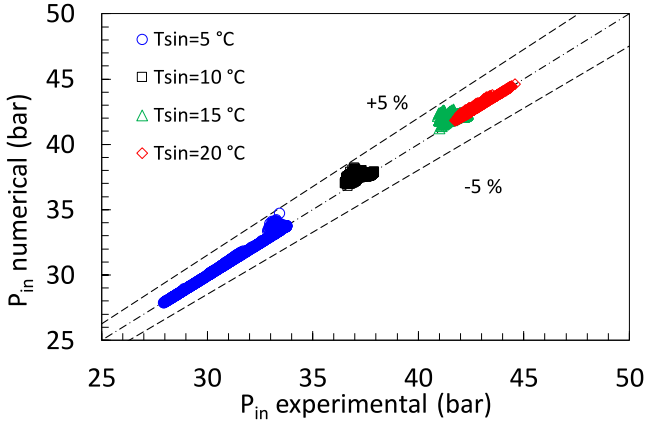

Fig. 9. Refrigerant inlet pressure.

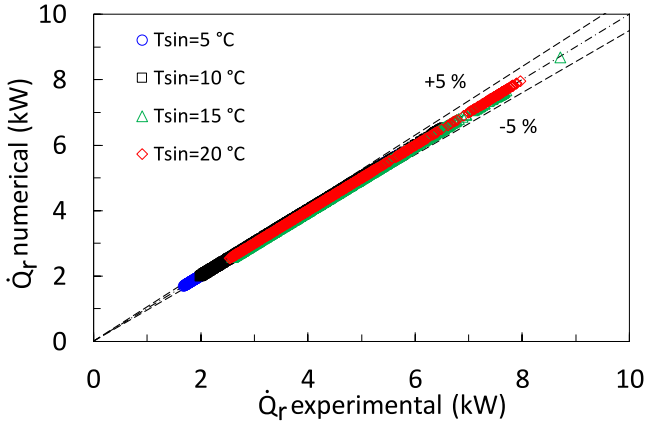

Fig. 10. Heat transfer rate.

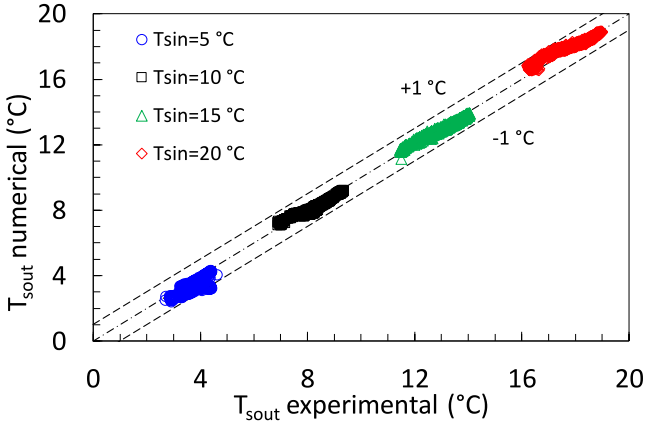

Fig. 11. Secondary fluid outlet temperature.

which is compared with the real one. This allows the behavior of the exchanger to be modeled iteratively. The numerical method has been contrasted by using a database of 366 experimental data obtained under stationary test conditions, some of them performed in our laboratory, and the others are taken from the open literature. These data correspond to six different refrigerants (R134a, R1234yf, R513A, R507A, R290, and R744), eight different plate heat exchangers, and variable operating conditions (different superheating degree, secondary fluid flow rate, or inlet quality).

In parallel to this development, three different HTC correlations have been analyzed. According to the results obtained, all three correlations provide similar results. The results also showed the goodness and robustness of the method when predicting the different variables of interest.

Once the numerical method has been validated, it has been used to predict the performance of the evaporator under transient operating conditions. The high accuracy in the prediction of the main variables of interest, demonstrates the ability of the method to be used for transient analysis of refrigeration systems.

Further work includes the development of a similar numerical method for condensers, gas coolers, and internal heat exchangers, and its coupling with a model for the compressor, which can be easily developed from the AHRI correlations usually provided by the manufacturers, in order to develop a model for a whole refrigeration system, that can be used to simulate its behavior during long transient processes.

Declaration of competing interest

The authors declare that they have no known competing financial interests or personal relationships that could have appeared to influence the work reported in this paper.

Data availability

Data will be made available on request.

Acknowledgement

The work in this paper has been financed by the Spanish Ministry of Science and Innovation under Project TED2021-131173B–I00 and the NextGenerationEU recovery plan.

References

[1] R.K. Shah, D.P. Sekuli, Fundamentals of Heat Exchanger Design, John Wiley & Sons, Inc., Hoboken, NJ, USA, 2003, https://doi.org/10.1002/9780470172605.

[2] J.J. Klemes, O. Arsenyeva, P. Kapustenko, L. Tovazhnyanskyy, Compact Heat Exchangers for Energy Transfer Intensification: Low Grade Heat and Fouling Mitigation, CRC Press, Boca Raton, 2016, https://doi.org/10.1201/b18862.

[3] T. Bentaleb, M.T. Pham, D. Eberard, W. Marquis-Favre, Bond Graph Model of A Water Heat Exchanger, ECMS 2016 Proceedings Edited by Thorsten Claus, Frank Herrmann, Michael Manitz, Oliver Rose, 2016. https://www.academia.edu/25326122/Bond_Graph_Model_of_a_Water_Heat_Exchanger. (Accessed 13 October 2022). accessed.

[4] M. Kebdani, G.D. Tanguy, A. Dazin, P. Dupont, Experimental development and bond graph dynamic modelling of a brazed plate heat exchanger, Int. J. Simul. Process Model. 12 (2017) 249.

[5] J.B. Nielsen, E. Pedersen, On the modelling of heat exchangers and heat exchanger network dynamics using bond graphs, Math. Comput. Model. Dyn. Syst. 24 (2018) 626–642, https://doi.org/10.1080/13873954.2018.1533566.

[6] J. Lee, P.A. Domanski, Impact of Air and Refrigerant Maldistributions on the Performance of Finned-Tube Evaporators with R-22 and R-407C, 1997. https://www.nist.gov/publications/impact-air-and-refrigerant-maldistributions-performance-finned-tube-evaporators-r-22. (Accessed 20 April 2022). accessed.

[7] J.M. Corberán, P. Fernández de Córdoba, J. Gonzálvez, F. Alias, Semiexplicit method for wall temperature linked equations (SEWTLE): a general finite-volume technique for the calculation of complex heat exchangers, Numer. Heat Tran., Part B: Fundamentals. 40 (2001) 37–59, https://doi.org/10.1080/104077901300233596.

[8] H. Jiang, Development of a Simulation and Optimization Tool for Heat Exchanger Design, University of Maryland, 2003. http://hdl.handle.net/1903/3676.

[9] H. Jiang, V. Aute, R. Radermacher, CoilDesigner: a general-purpose simulation and design tool for air-to-refrigerant heat exchangers, Int. J. Refrig. 29 (2006) 601–610, https://doi.org/10.1016/j.ijrefrig.2005.09.019.

[10] P.A. Domanski, D.A. Yashar, J. Wojtusiak, EVAP-COND, 2020. https://www.nist.gov/services-resources/software/evap-cond-version-50. (Accessed 21 April 2022). accessed.

[11] IMST-ART, A Simulation Tool to Assist the Selection, Design and Optimization of Refrigeration Equipment and Components, 2021. https://www.imst-art.com/.

[12] A. CoilDesigner, Highly Customizable Software Tool for the Design, Simulation and Optimization of Air-To-Refrigerant Heat Exchangers, 2016. https://optimizedthermalsystems.com/index.php/products/coildesigner. (Accessed 21 April 2022). accessed.

[13] M.-H. Kim, C.W. Bullard, Development of a microchannel evaporator model for a CO_2 air-conditioning system, Energy 26 (2001) 931–948, https://doi.org/10.1016/S0360-5442(01)00042-1.

[14] J.M. Yin, C.W. Bullard, P.S. Hrnjak, R-744 gas cooler model development and validation, Int. J. Refrig. 24 (2001) 692–701, https://doi.org/10.1016/S0140-7007(00)00082-7.

[15] P. Asinari, L. Cecchinato, E. Fornasieri, Effects of thermal conduction in microchannel gas coolers for carbon dioxide, Int. J. Refrig. 27 (2004) 577–586, https://doi.org/10.1016/j.ijrefrig.2004.04.001.

[16] J.R. García-Cascales, F. Vera-García, J. González-Maciá, J.M. Corberán-Salvador, M.W. Johnson, G.T. Kohler, On the analysis of compact heat exchangers working as evaporators, in: RCR 2009. 1st IIR Workshop on Refrigerant Charge Reduction in Refrigerating Systems, Antony, France, 2009. https://iifiir.org/en/fridoc/on-the-analysis-of-compact-heat-exchangers-working-as-evaporators-26092. (Accessed 21 April 2022). accessed.

[17] J.R. García-Cascales, F. Vera-García, J. González-Maciá, J.M. Corberán-Salvador, M.W. Johnson, G.T. Kohler, Compact heat exchangers modeling: Condensation, Int. J. Refrig. 33 (2010) 135–147, https://doi.org/10.1016/j.ijrefrig.2009.08.013.

[18] Mpower. Modine's custom vapor compression system design, (n.d.). https://www.modine.com/.

[19] B.M. Fronk, S. Garimella, Water–coupled carbon dioxide microchannel gas cooler for heat pump water heaters: Part II – model development and validation, Int. J. Refrig. 34 (2011) 17–28, https://doi.org/10.1016/j.ijrefrig.2010.05.012.

[20] S. Martínez Ballester, Numerical Model for Microchannel Condensers and Gas Coolers with an Improved Air-Side Approach, Tesis doctoral, Universitat Politècnica de València, 2012, https://doi.org/10.4995/Thesis/10251/17453.

[21] J. Corberán, J. Gonzálvez, P. Montes, R. Blasco, 'ART' A computer code to assist the design of refrigeration and A/C equipment, in: International Refrigeration and Air Conditioning Conference, 2002. https://docs.lib.purdue.edu/iracc/570.

[22] H. Qiao, V. Aute, H. Lee, K. Saleh, R. Radermacher, A new model for plate heat exchangers with generalized flow configurations and phase change, Int. J. Refrig. 36 (2013) 622–632, https://doi.org/10.1016/j.ijrefrig.2012.11.020.

[23] R. Eldeeb, V. Aute, R. Radermacher, An improved approach for modeling plate heat exchangers based on successive substitution in alternating flow directions, in: 16th International Refrigeration and Air Conditioning Conference at Purdue, IN, USA, July 11-14, 2016, p. 9, 2279, https://docs.lib.purdue.edu/cgi/viewcontent.cgi?article=2683&context=iracc.

[24] V.S. Gullapalli, Estimation of Thermal and Hydraulic Characteristics of Compact Brazed Plate Heat Exchangers, Lund University, 2013. https://www.energy.lth.se/fileadmin/energivetenskaper/Avhandlingar/Vijaya_PhD_Final_Thesis_V07May2013.pdf.

[25] Swep SSP G8, (n.d.). https://www.swep.net/support/ssp-calculation-software/ssp-g8/.

[26] PhD. Gullapalli Vijaya Sekhar, Modeling of brazed plate heat exchangers for ORC systems, Energy Proc. 129 (2017) 443–450, https://doi.org/10.1016/j.egypro.2017.09.207.

[27] W. Yoon, J.H. Jeong, Development of a numerical analysis model using a flow network for a plate heat exchanger with consideration of the flow distribution, Int. J. Heat Mass Tran. 112 (2017) 1–17, https://doi.org/10.1016/j.ijheatmasstransfer.2017.04.087.

[28] H. Jeong, J. Oh, H. Lee, Experimental investigation of performance of plate heat exchanger as organic Rankine cycle evaporator, Int. J. Heat Mass Tran. 159 (2020) 120158, https://doi.org/10.1016/j.ijheatmasstransfer.2020.120158.

[29] M. Fratczak, P. Nowak, J. Czeczot, M. Metzger, Simplified dynamical input–output modeling of plate heat exchangers – case study, Appl. Therm. Eng. 98 (2016) 880–893, https://doi.org/10.1016/j.applthermaleng.2016.01.004.

[30] Y. Wang, S. You, W. Zheng, H. Zhang, X. Zheng, Q. Miao, State space model and robust control of plate heat exchanger for dynamic performance improvement, Appl. Therm. Eng. 128 (2018) 1588–1604, https://doi.org/10.1016/j.applthermaleng.2017.09.120.

[31] K.-L. He, Q. Chen, Y.-T. Liu, J.-H. Hao, Y.-F. Wang, Y. Yuan, A transient heat current model for dynamic performance analysis and optimal control of heat transfer system, Int. J. Heat Mass Tran. 145 (2019), 118767, https://doi.org/10.1016/j.ijheatmasstransfer.2019.118767.

[32] P.Z. Csurcsia, J. Decuyper, A.M. Chaudhry, T. De Troyer, S. Bram, Nonlinear modeling of a plate heat exchanger of a district heating system, IFAC-PapersOnLine 55 (2022) 747–752, https://doi.org/10.1016/j.ifacol.2022.07.402.

[33] B.D. Raja, R.L. Jhala, V. Patel, Thermal–hydraulic optimization of plate heat exchanger: a multi–objective approach, Int. J. Therm. Sci. 124 (2018) 522–535, https://doi.org/10.1016/j.ijthermalsci.2017.10.035.

[34] H. Shokouhmand, M. Hasanpour, Effect of flow maldistribution on the optimal design of plate heat exchanger using constrained multi objective genetic algorithm, Case Stud. Therm. Eng. 18 (2020), 100570, https://doi.org/10.1016/j.csite.2019.100570.

[35] S. Dinesh Kumar, D. Chandramohan, K. Purushothaman, T. Sathish, Optimal hydraulic and thermal constrain for plate heat exchanger using multi objective wale optimization, Mater. Today Proc. 21 (2020) 876–881, https://doi.org/10.1016/j.matpr.2019.07.710.

[36] A.L.M. Nahes, M.J. Bagajewicz, A.L.H. Costa, Simulation of gasketed-plate heat exchangers using a generalized model with variable physical properties, Appl. Therm. Eng. 217 (2022) 119197, https://doi.org/10.1016/j.applthermaleng.2022.119197.

[37] G. Starace, M. Fiorentino, M.P. Longo, E. Carluccio, A hybrid method for the cross flow compact heat exchangers design, Appl. Therm. Eng. 111 (2017) 1129–1142, https://doi.org/10.1016/j.applthermaleng.2016.10.018.

[38] G. Starace, M. Fiorentino, B. Meleleo, C. Risolo, The hybrid method applied to the plate-finned tube evaporator geometry, Int. J. Refrig. 88 (2018) 67–77, https://doi.org/10.1016/j.ijrefrig.2017.12.007.

[39] M. Fiorentino, G. Starace, The design of countercurrent evaporative condensers with the hybrid method, Appl. Therm. Eng. 130 (2018) 889–898, https://doi.org/10.1016/j.applthermaleng.2017.11.076.

[40] J.M. Corberán, J. Gonzálvez, D. Fuentes, Calculation of refrigerant properties by linear interpolation of bidimensional meshes, in: commercial refrigeration. Thermophysical properties and transfer processes of refrigerants, in: Proceedings of the IIR International Conferences, 2005. https://iifiir.org/en/fridoc/calculation-of-refrigerant-properties-by-linear-interpolation-of-22099. (Accessed 20 April 2022). accessed.

[41] E.W. Lemmon, M.L. Huber, M.O. McLinden, NIST Standard Reference Database 23: Reference Fluid Thermodynamic and Transport Properties-REFPROP, Version 10.0, National Institute of Standards and Technology, Standard Reference Data Program, 2018, https://doi.org/10.18434/T4/1502528.

[42] J.R. Simon, T.M. Bandhauer, An experimentally validated evaporative phase change heat transfer model for low mass flux applications using R134a in plate heat exchangers, Int. J. Refrig. 131 (2021) 604–614, https://doi.org/10.1016/j.ijrefrig.2021.08.003.

[43] J. Claesson, Thermal and Hydraulic Characteristics of Brazed Plate Heat Exchangers. Part I: Review of Single–phase and Two–phase Adiabatic and Flow Boiling Characteristics, 2005. Orlando, FL, USA, https://www.techstreet.com/ashrae/standards/ashrae-transactions-2005-winter-meeting-orlando-fl-volume-111-part-1?gateway_code=ashrae&product_id=1703528#jumps. #OR–05–10–2.

[44] J.R. García-Cascales, F. Vera-García, J.M. Corberán-Salvador, J. González-Maciá, Assessment of boiling and condensation heat transfer correlations in the modelling of plate heat exchangers, Int. J. Refrig. 30 (2007) 1029–1041, https://doi.org/10.1016/j.ijrefrig.2007.01.004.

[45] R.L. Amalfi, F. Vakili-Farahani, J.R. Thome, Flow boiling and frictional pressure gradients in plate heat exchangers. Part 1: review and experimental database, Int. J. Refrig. 61 (2016) 166–184, https://doi.org/10.1016/j.ijrefrig.2015.07.010.

[46] R.L. Amalfi, F. Vakili-Farahani, J.R. Thome, Flow boiling and frictional pressure gradients in plate heat exchangers. Part 2: comparison of literature methods to database and new prediction methods, Int. J. Refrig. 61 (2016) 185–203, https://doi.org/10.1016/j.ijrefrig.2015.07.009.

[47] P.A. Kew, K. Cornwell, Correlations for the prediction of boiling heat transfer in small-diameter channels, Appl. Therm. Eng. 17 (1997) 705–715, https://doi.org/10.1016/S1359-4311(96)00071-3.

[48] G.A. Longo, S. Mancin, G. Righetti, C. Zilio, A new model for refrigerant boiling inside Brazed Plate Heat Exchangers (BPHEs), Int. J. Heat Mass Tran. 91 (2015) 144–149, https://doi.org/10.1016/j.ijheatmasstransfer.2015.07.078.

[49] M.G. Cooper, Heat flow rates in saturated nucleate pool boiling-a wide-ranging examination using reduced properties, in: J.P. Hartnett, T.F. Irvine (Eds.), Advances in Heat Transfer, Elsevier, 1984, pp. 157–239, https://doi.org/10.1016/S0065-2717(08)70205-3.

[50] J. Claesson, Thermal and Hydraulic Performance of Compact Brazed Plate Heat Exchangers Operating as Evaporators in Domestic Heat Pumps, KTH, School of Industrial Engineering and Management (ITM), Energy Technology, 2005. http://urn.kb.se/resolve?urn=urn:nbn:se:kth:diva-110. (Accessed 21 April 2022). accessed.

[51] G.A. Longo, A. Gasparella, HFC-410A vaporisation inside a commercial brazed plate heat exchanger, Exp. Therm. Fluid Sci. 32 (2007) 107–116, https://doi.org/10.1016/j.expthermflusci.2007.02.004.

[52] G.A. Longo, Vaporisation of the low GWP refrigerant HFO1234yf inside a brazed plate heat exchanger, Int. J. Refrig. 35 (2012) 952–961, https://doi.org/10.1016/j.ijrefrig.2011.12.012.

[53] L. Wang, R. Christensen, B. Sunden, Calculation Procedure for Steam Condensation in Plate Heat Exchangers, Compact Heat Exchangers and Enhancement Technology for the Process Industries, 1999, in: https://www.begellhouse.com/books/compact-heat-exchangers-and-enhancement-technology-for-the-process-industries-2003.html. (Accessed 21 April 2022). accessed.

[54] A. Jokar, M.H. Hosni, S.J. Eckels, Dimensional analysis on the evaporation and condensation of refrigerant R-134a in minichannel plate heat exchangers, Appl. Therm. Eng. 26 (2006) 2287–2300, https://doi.org/10.1016/j.applthermaleng.2006.03.015.

[55] J. Huang, T.J. Sheer, M. Bailey-McEwan, Heat transfer and pressure drop in plate heat exchanger refrigerant evaporators, Int. J. Refrig. 35 (2012) 325–335, https://doi.org/10.1016/j.ijrefrig.2011.11.002.

[56] F. Illán-Gómez, J.R. García-Cascales, Experimental comparison of an air-to-water refrigeration system working with R134a and R1234yf, Int. J. Refrig. 97 (2019) 124–131, https://doi.org/10.1016/j.ijrefrig.2018.09.026.

[57] F.J.S. Velasco, F. Illán-Gómez, J.R. García-Cascales, Energy efficiency evaluation of the use of R513A as a drop-in replacement for R134a in a water chiller with a minichannel condenser for air-conditioning applications, Appl. Therm. Eng. 182 (2021), 115915, https://doi.org/10.1016/j.applthermaleng.2020.115915.

[58] F. Illán-Gómez, V.F. Sena-Cuevas, J.R. García-Cascales, F.J.S. Velasco, Analysis of the optimal gas cooler pressure of a CO_2 heat pump with gas bypass for hot water generation, Appl. Therm. Eng. 182 (2021), 116110, https://doi.org/10.1016/j.applthermaleng.2020.116110.

[59] F. Illán-Gómez, V.F. Sena-Cuevas, J.R. García-Cascales, F.J.S. Velasco, Experimental and numerical study of a CO_2 water-to-water heat pump for hot water generation, Int. J. Refrig. 132 (2021) 30–44, https://doi.org/10.1016/j.ijrefrig.2021.09.020.

[60] O.I. Martínez Galván, Estudio experimental de optimización de una bomba de calor agua–agua empleando propano como fluido de trabajo, Tesis doctoral, Universitat Politècnica de València, 2008, https://doi.org/10.4995/Thesis/10251/3344.

[61] J. Huang, Performance Analysis of Plate Heat Exchangers Used as Refrigerant Evaporators, Thesis, Faculty of Engineering and the Built Environment, University of the Witwatersrand, 2011. http://wiredspace.wits.ac.za/handle/10539/9779. (Accessed 21 April 2022). accessed.

[62] S.W. Churchill, Friction factor equation spans all fluid flow regimes, Chem. Eng. (1977) 91–92.

[63] F.J.S. Velasco, M.R. Haddouche, F. Illán-Gómez, J.R. García-Cascales, Experimental characterization of the coupling and heating performance of a CO_2 water-to-water heat pump and a water storage tank for domestic hot water production system, Energy Build. 265 (2022), 112085, https://doi.org/10.1016/j.enbuild.2022.112085.